ELSEVIER

Optics and Lasers in Engineering 37 (2002) 553–563

OPTICS and LASERS in ENGINEERING

Generation of tunable green radiation in bulk periodically poled $KTiOPO_4$

P. Zeppini[a], P. Cancio[b,*], G. Giusfredi[b], D. Mazzotti[a,b], A. Arie[c], G. Rosenman[c], P. De Natale[b]

[a] *European Laboratory for Nonlinear Spectroscopy, and Department of Physics, University of Firenze, Largo E. Fermi, 2 I-50125 Firenze, Italy*

[b] *Istituto Nazionale di Ottica Applicata, Largo E. Fermi, 6 I-50125 Firenze, Italy*

[c] *Department of Electrical Engineering—Physical Electronics, Faculty of Engineering, Tel Aviv University, 69978 Tel Aviv, Israel*

Received 2 February 2001; received in revised form 20 April 2001; accepted 23 April 2001

Abstract

We report a characterisation of a flux-grown periodically poled $KTiOPO_4$ crystal used for second-harmonic generation in a diode laser source, that operates with fundamental radiation tunable around 1083 nm wavelength. The conversion efficiency is measured for the three different grating periods of the crystal, as a function of input wavelength, crystal temperature and fundamental power. The measurements were fitted to the theoretical model of Boyd and Kleinman for frequency conversion of focused Gaussian beams. This enabled us to determine the temperature and wavelength dependence of the difference in refractive index between the interacting waves.

Keywords: Periodically poled crystal; Second-harmonic generation; Non-linear optical coefficient; KTP

1. Introduction

Progress in the development of periodically poled (PP) materials is making possible a wider diffusion of quasi-phase-matching (QPM) techniques, in place of the

*Corresponding author. Fax: +39-055-233-7755.
E-mail address: pcp@ino.it (P. Cancio).

0143-8166/02/$ - see front matter
PII: S0143-8166(01)00138-5

more traditional birefringent-phase-matching [1]. QPM offers several advantages, like non-critical phase-matching of the non-linear process throughout the whole crystal transparency range at any given temperature, a larger frequency conversion efficiency and increased tolerance to wavelength and temperature variations. Pioneering work on QPM was mainly focused on $LiNbO_3$ (LN), although other ferroelectric materials, like $KTiOPO_4$ (KTP), have been more recently developed for QPM. In spite of the lower conversion efficiency, in comparison with PP-LN, PP-KTP has a higher resistance to photorefractive damage, that allows operation around room temperature even at visible wavelengths. Furthermore, short domain periods seem to be easier to fabricate in KTP than in LN [1,2]. In addition, PP-KTP is less sensitive to thermal induced distortions such as thermal lensing.

Second-harmonic generation (SHG) in PP-KTP has already been demonstrated for cw sources like Nd-YAG at 1064 nm [3–5] or, near 780 nm, for radiation from a Ti : Sa laser [4,6]. More recently, sub-Doppler spectroscopy of I_2 lines around 541 nm has been performed using a 1083 nm diode laser in combination with a PP-KTP crystal for frequency doubling, for which a continuous tunability of about 1.2 THz in the green has been demonstrated [7]. The application to saturation spectroscopy of such a widely tunable source requires a full characterisation of the crystal doubling efficiency with respect to all parameters. In this paper, we report a detailed study of second-harmonic conversion efficiency, in the 541 nm region, for a single PP-KTP crystal containing three poling gratings of different periodicity. In particular, the doubling efficiency as a function of input wavelength, crystal temperature and input power is studied.

2. The experimental set-up

The experimental set-up of the system consists of two main parts (Fig. 1): the infrared laser source and the KTP crystal. The laser source is a fibre amplified distributed-Bragg-reflector (DBR) diode laser emitting at 1083 nm. The diode laser is mounted in an extended cavity configuration to reduce the linewidth up to about 300 kHz [8]. In this configuration, a maximum output power of 25 mW is available. In order to increase the green power after the doubling process, this infrared light is amplified using a commercial ytterbium-doped fibre amplifier (YDFA) with 30 dB of maximum gain and an output saturation power of 1.2 W at 1083 nm [9].

The crystal is a flux-grown PP-KTP. It is 10 mm long, 8 mm wide and 0.6 mm thick, and there are three different domains with different poling grating periods: $\Lambda_1 = 9.48\,\mu m$, $\Lambda_2 = 9.50\,\mu m$ and $\Lambda_3 = 9.52\,\mu m$. The crystal was periodically poled using the low-temperature electric field poling technique [10]. The ferroelectric domain inversion allows the reversal of the sign of the non-linear coefficient d_{33}, the largest in the KTP crystal. Consequently, the amplified infrared radiation must be s-polarised for efficient SHG. A combination of a quarter-wave and a half-wave plate on the injected radiation (Fig. 1), together with the retardation introduced by

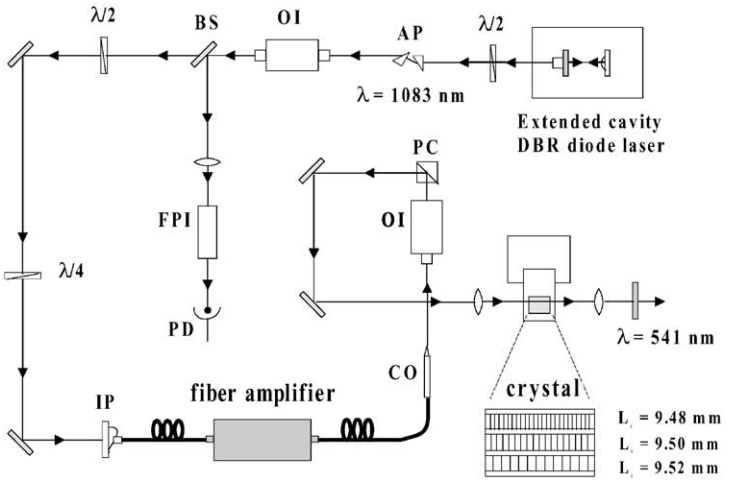

Fig. 1. The experimental set-up. BS: beam splitter, AP: anamorphic prisms, OI: optical isolator, IP: fibre input port, CO: fibre output collimator, PC: polarising cube, FPI: Fabry–Perot interferometer and PD: photodiode.

the fibre, define the required s-polarisation at the fibre amplifier output. Two optical isolators, before and after the fibre amplifier (30 dB isolation each), avoid unwanted optical feedback onto the laser from the amplifier and the PP crystal, respectively.

The amplifier output radiation is a Gaussian beam; the beam waist after the optical isolator is approximately circular with a measured diameter of 142.5 μm. In order to maximise second-harmonic generated power, the infrared light is focused into the crystal by using a lens with 50 mm focal length.

The crystal is located in a copper housing with a temperature fixed by a thermoelectric device, a NTC (negative temperature coefficient) thermistor and a controller. With this system, the crystal temperature is stabilised with an uncertainty of 0.3 K. The absolute temperature is independently measured using another temperature sensor (Type K Fluke 51). The whole system is mounted on a *three-axis stage assembly*, that allows to align the crystal with respect to the laser beam.

The output light from the crystal is collimated using a lens with 100 mm focal length which is A/R coated at 541 nm. The green light is filtered out from the fundamental radiation using a bandpass filter.

In order to characterise the PP-KTP crystal, a calibrated silicon detector (Coherent mod. LM-2) was used to measure the green and the infrared power at values up to 10 mW. A thermal detector (Coherent mod. LM-10) was used to measure the fundamental power at values above 10 mW. Finally, a Michelson-type wave-meter (accuracy $1:10^6$) was used to measure the infrared and green radiation wavelengths.

3. Results

3.1. Measurements of the doubling efficiency

We have characterised the doubling efficiency of the PP-KTP crystal as a function of the fundamental power and wavelength, as well as the crystal operating temperature.

By measuring the green power at different infrared power levels, we calculated the internal doubling efficiency for the three domains of the KTP crystal. Fig. 2 shows the measured green power vs. the squared fundamental power for all three domains. For all three series of measurements, the fundamental radiation wavelength was fixed at $\lambda = 1083.272$ nm, while the crystal temperature was set to the optimal value for each domain. The measured power levels are corrected on the basis of the Fresnel reflection losses. These losses amount to 8.59% for the fundamental radiation at the input facet and 9.43% for the second harmonic at the output facet. Losses of 3% and 11.3%, measured respectively on the L_2 lens and on the filter for the doubled radiation, are also considered. Finally, an offset in the green power, due to the 1.5×10^{-3}% of the unfiltered infrared radiation, is subtracted. The main contribution to the uncertainty on the fundamental power comes from the detector read-out and is about 1 mW. The uncertainty on the second-harmonic power value is 4%, due to slow crystal temperature fluctuations, having a time scale of a few seconds.

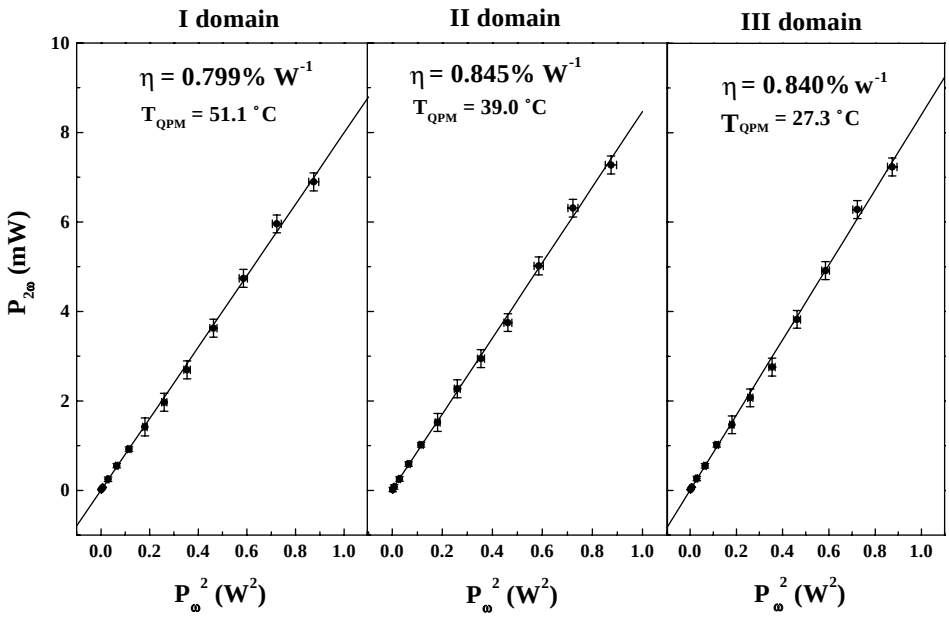

Fig. 2. The experimental SHG efficiency for the three crystal domains. The data are fitted with a linear curve.

The internal normalised doubling efficiency $\eta \equiv P^{2\omega}/(P^{\omega})^2$ is obtained from a linear fit of the experimental data. The $0.008\%\,\mathrm{W}^{-1}$ uncertainty on the efficiency values comes from the fit considering the error bars of the fundamental and green power data. As we can see in Fig. 2, two of the three measured values for the efficiency are consistent, while the value obtained for the domain with a grating period $\Lambda_1 = 9.48\,\mu\mathrm{m}$ is smaller by a 5% factor. This can be due to inhomogeneities of the ferroelectric domains. From the other two measurements we can deduce the value $\eta = (8.40 \pm 0.08) \times 10^{-3}\,\mathrm{W}^{-1}$ for the internal doubling efficiency of the KTP crystal, with a maximum green power of 5.8 mW for 1 W input power at 1083 nm.

The theoretical conversion efficiency is [11]

$$\eta \equiv \frac{P^{2\omega}}{(P^{\omega})^2} = \frac{16\pi^2 L}{\lambda^3 n_1 n_2 \varepsilon_0 c} d_{\mathrm{eff}}^2 h(\xi, \sigma), \tag{1}$$

where λ and P^{ω} are respectively the wavelength and the power of the fundamental radiation, L is the crystal length, n_1 and n_2 are the indices of refraction for the fundamental and for the second harmonic, respectively, c is the speed of light, ε_0 is the vacuum permittivity, $h(\xi, \sigma)$ is the Boyd–Kleinman focusing factor, that depends on the focusing parameter ξ and on the normalised phase mismatch $\sigma = -\Delta k L/2\xi$, where $\Delta k \equiv k^{2\omega} - 2k^{\omega} - 2\pi m/\Lambda$, m being an integer that denotes the QPM order. The maximum value for h is 1.068, when $\xi = 2.84$ and σ is a convenient value between 0 and 1 [11].

For our set-up, we calculate $\xi = 4.15$ and $h = 1.0259$, from the fit of the second-harmonic power vs. crystal temperature and fundamental wavelength (see Section 3.2). The QPM effective non-linear coefficient is [1]

$$d_{\mathrm{eff}} = \frac{2}{\pi m} \sin(\pi m D) d_{33}, \tag{2}$$

where the "duty cycle" D is the ratio between the length of the inverted ferroelectric domain and the grating period. In our crystal, $m = 1$ and the optimal duty cycle is $D = 0.5$, giving $d_{\mathrm{eff}} = 2d_{33}/\pi$. Therefore, from Eq. (1), we can calculate the non-linear coefficient d_{33} using the formula

$$d_{33} = \frac{1}{8} \sqrt{\frac{\lambda^3 n_1 n_2 \varepsilon_0 c}{L h(\xi, \sigma)}}\, \eta, \tag{3}$$

obtaining a value of $d_{33} = (12.20 \pm 0.06)\,\mathrm{pm/V}$ by introducing the measured efficiency value, defined above, and the values of the other parameters in our experiment. Note that this value represents a lower limit on the non-linear coefficient, since any imperfection in the beam shape, duty cycle or periodic domain structure, will reduce the conversion efficiency.

3.2. Phase matching parameters tuning measurements

The first order QPM condition for optimum SHG with a focused Gaussian light beam is [11]

$$0<\sigma=\frac{L}{2\xi}\left(\frac{4\pi}{\lambda}[n_{\omega}(T,\lambda)-n_{2\omega}(T,\lambda)]+\frac{2\pi}{\Lambda}\right)<1 \tag{4}$$

and, for a given crystal of length L, depends on four parameters, namely the fundamental wavelength λ, the crystal temperature T, the grating period Λ and the focusing ξ. We studied the SHG process varying both T and λ in a wide interval for the three available grating periods.

3.2.1. Temperature tuning

The temperature tuning analysis was made with two different approaches: the first set of measurements was performed by keeping the wavelength constant to the value $\lambda = 1083.272$ nm for the three different domains (Fig. 3a), while the second set involves just one domain ($\Lambda = 9.50\,\mu$m) at three different wavelengths of the fundamental radiation (Fig. 3b). In all cases, the second-harmonic power is depicted as a function of the crystal relative temperature, that is the difference between the crystal temperature and the optimal phase-matching temperature (T_{QPM}). T_{QPM} is unambiguously defined when the grating period is chosen and the wavelength is fixed. We obtained $T_{\mathrm{QPM}} = 51.1^{\circ}$C, 39.0°C and 27.3°C, respectively, for periods $\Lambda = 9.48$, 9.50 and 9.52 μm in Fig. 3a, and $T_{\mathrm{QPM}} = 47.3^{\circ}$C, 36.3°C and 27.6°C, respectively, for wavelengths $\lambda_{\mathrm{QPM}} = 1083.79$, 1083.05 and 1082.56 nm in Fig. 3b. We can observe that the phase-matching temperature full-width at half-maximum (FWHM) ΔT is more or less constant for all curves of Fig. 3.

3.2.2. Wavelength tuning

The wide tunability range of the diode laser source allowed us to reconstruct the whole efficiency profile by varying the fundamental wavelength. The measurement scheme is similar to that used for recording the temperature tuning curves. First, we record the second-harmonic power as a function of the wavelength for all three different domains, at a fixed temperature of the crystal. Then, we change the temperature and the same set of measurements is repeated for a total of three different temperatures. In Fig. 4, we show seven of the nine possible wavelength-efficiency curves: it was impossible to reconstruct entirely the other two curves, due to the tuning limits imposed by the source. If these curves are compared with those in Fig. 3, it can be noticed that the profile is reversed, with respect to the horizontal axis, because the mismatch varies in a different way if either the crystal temperature T or the wavelength λ is varied.

Regarding the wavelength behaviour, it can be seen, in Fig. 4, that the FWHM $\Delta\lambda$ is the same for all curves. This is an indication that, for the range of variation of λ and T, the dependence of the difference, Δn, between the value of the refractive index at 1083 nm and at the second-harmonic frequency is linear for the T and λ ranges investigated. The following expression for Δn was assumed:

$$\Delta n(T,\lambda) = [n_{2\omega}(T,\lambda) - n_{\omega}(T,\lambda)] = \Delta n_0 + B_T(T - T_0) + B_{\lambda}(\lambda - \lambda_0), \tag{5}$$

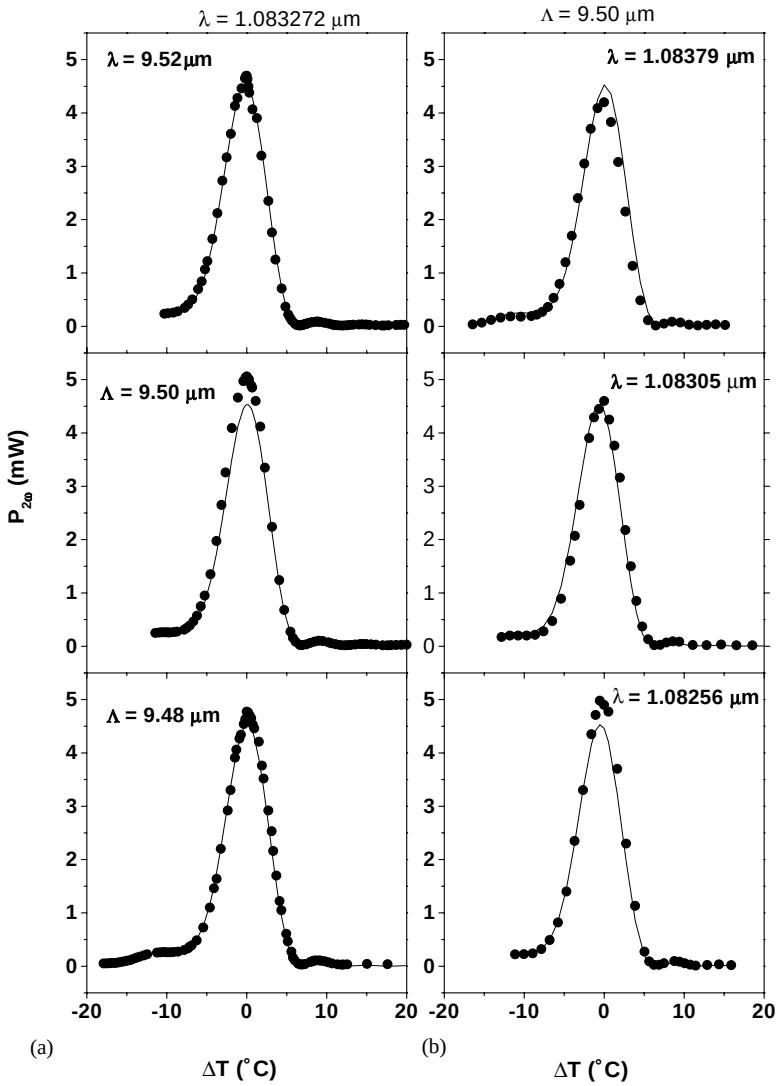

Fig. 3. The SHG phase matching curves as a function of crystal temperature at (a) constant fundamental wavelength $\lambda = 1083.272$ nm and (b) constant poling period $\Lambda = 9.50$ μm. Circle points: experimental data, solid line: fit to the function of Eq. (6).

where Δn_0 is the value of Δn calculated at $T_0 = 25^\circ$C and $\lambda_0 = 1.083$ μm, B_T and B_λ are the linear coefficients in T and λ, respectively. We neglected the dependence of the poling period Λ on temperature. The parameters in Eq. (5) can be calculated by fitting all the experimental data in Figs. 3 and 4 to the function $P_{2\omega} = \eta P_\omega^2$:

$$P_{2\omega}(T, \lambda; A, \Delta n_0, B_T, B_\lambda, \xi) = Ah(\sigma, \xi) = \frac{A}{4\xi}\left(\int_{-\xi}^{\xi} \frac{e^{i\sigma(T,\lambda;\Delta n_0, B_T, B_\lambda, \xi)\tau}}{1 + i\tau} d\tau\right)^2, \qquad (6)$$

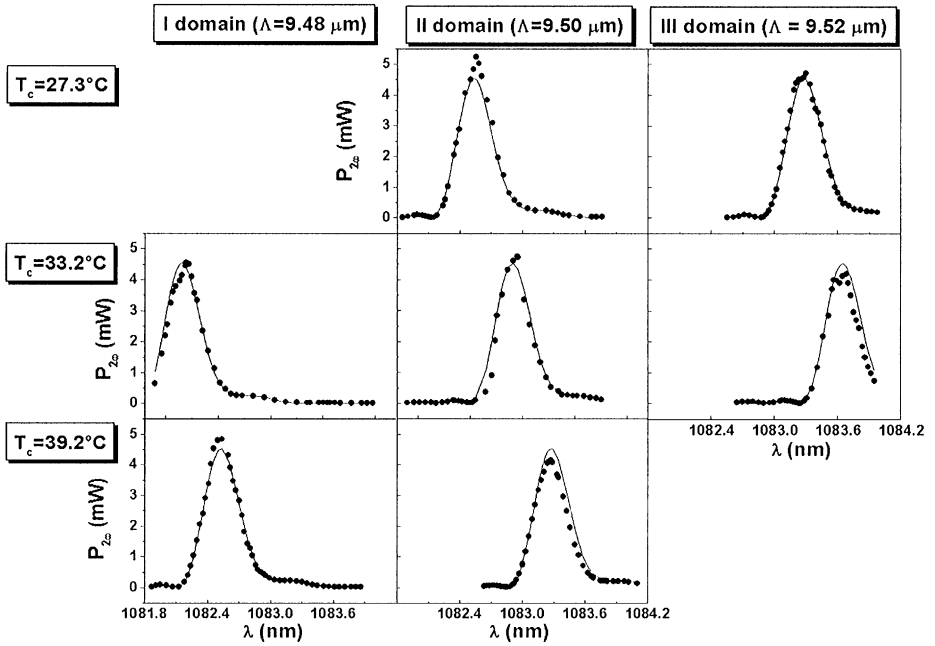

Fig. 4. The SHG phase matching curves as a function of fundamental wavelength. Circle points: experimental data, solid line: fit to the function of Eq. (6).

where A is a parameter that takes into account the amplitude of the signal, that depends on the fundamental power P_ω. The focusing parameter ξ was left as free parameter in the fit because the experimental determinations did not provide results with the accuracy required to reproduce the asymmetric behaviour of the curves in Figs. 3 and 4.

The least squares fit results for the parameters gave: $A = (4.42 \pm 0.06)\,\mathrm{mW}$, $\Delta n_0 = (0.056870 \pm 0.000002)$, $B_T = (9.981 \pm 0.008) \times 10^{-6}(^\circ\mathrm{C})^{-1}$, $B_\lambda = (-0.108 \pm 0.001)\,\mu\mathrm{m}^{-1}$ and $\xi = (4.15 \pm 0.04)$. The fitted curves are shown in Figs. 3 and 4 together with the experimental data. A very good agreement is obtained in all cases.

From the fitted parameters, the acceptance wavelength and temperature bands can be calculated by considering the value of $\Delta\sigma_{1/2} = \sigma_{1/2} - \sigma_{-1/2}$ for the σ values that satisfy the condition $h(\sigma_{\pm 1/2}, \xi) = h_{\max}/2$, and the first order expansion of σ with λ and T around the λ_{QPM} and T_{QPM} values for each curve:

$$\Delta\lambda = \Delta\sigma_{1/2} \frac{\xi\lambda_{\mathrm{QPM}}}{2\pi L} \left| -\frac{\Delta n(T_{\mathrm{QPM}}, \lambda_{\mathrm{QPM}})}{\lambda_{\mathrm{QPM}}} + B_\lambda \right|^{-1},$$

$$\Delta T = \Delta\sigma_{1/2} \frac{\xi\lambda_{\mathrm{QPM}}}{2\pi L} |B_T|^{-1}, \tag{7}$$

Table 1
Comparison of the $\Delta n(T,\lambda)$ parameters at 1083 nm and 25°C

	Ref. [12,13]	Ref. [14]	Ref. [15]	Ref. [16]	This work
Δn_0 [a]	0.05505	0.05713		0.05509	0.05687
$\frac{\partial}{\partial\lambda}\Delta n$ (μm^{-1}) [a]	−0.112	−0.114		−0.112	−0.108
$\frac{\partial}{\partial T}\Delta n$ ($10^{-6}(°C)^{-1}$) [b]	8.39		9.41	8.22	9.98

[a] Calculated from

$$\Delta n_0 = n\left(T,\frac{\lambda}{2}\right) - n(T,\lambda), \qquad \frac{\partial\Delta n}{\partial\lambda} = \frac{1}{2}\frac{\partial n(T,\lambda/2)}{\partial\lambda/2} - \frac{\partial n(T,\lambda)}{\partial\lambda},$$

with n from Sellmeier equations $n^2(\lambda)$ [12–14] and $n^2(T,\lambda)$ [16].
[b] Calculated from

$$\frac{\partial\Delta n}{\partial T} = \frac{\partial n(T,\lambda/2)}{\partial T} - \frac{\partial n(T,\lambda)}{\partial T},$$

with n from the Sellmeier equation $n^2(T,\lambda)$ [16], and calculated from the $dn/dT(\lambda)$ equations [12,15].

From these equations, $\Delta\lambda = (0.43 \pm 0.01)$ nm and $\Delta T = (6.9 \pm 0.1)$°C were obtained in all cases, confirming the linear dependence of Δn with λ and T.

We compared our results for $\Delta n(T,\lambda)$ with those that can be calculated from the Sellmeier equations, $n^2(T,\lambda)$, reported in literature [12–16]. The results are tabulated in Table 1. As we can see, there is a good agreement for all parameters.

It is worth noting that the determination of ξ from the fit is an accurate method to measure the waist of the fundamental laser beam in the crystal. In our experiment, the value measured for the waist was $w_0 = (15.0 \pm 0.1)\,\mu$m.

We also measured the "temperature–wavelength" characteristic of the crystal, under quasi-phase-matched conditions. As can be seen in Fig. 5, a linear behaviour was obtained in the range where data were taken. By fitting the experimental data to a straight line we measured a slope $\Delta\lambda/\Delta T|_{\mathrm{QPM}} \cong 0.06$ nm/°C.

4. Conclusions

In conclusion, we have fully characterised a PP-KTP crystal used for SHG with fundamental radiation at 1083 nm. The efficiency of the process was measured to be $8.4 \times 10^{-3}\,\mathrm{W}^{-1}$, which gives a non-linear second order coefficient of about 12 pm/V. The refractive index difference between 541.5 and 1083 nm was calculated as a linear function of the fundamental wavelength and crystal temperature. The $\Delta n(T,\lambda)$ dependence gives acceptance bandwidths for the SHG of about 0.4 nm and 7°C in wavelength and temperature, respectively. As is shown in Table 1, a good agreement

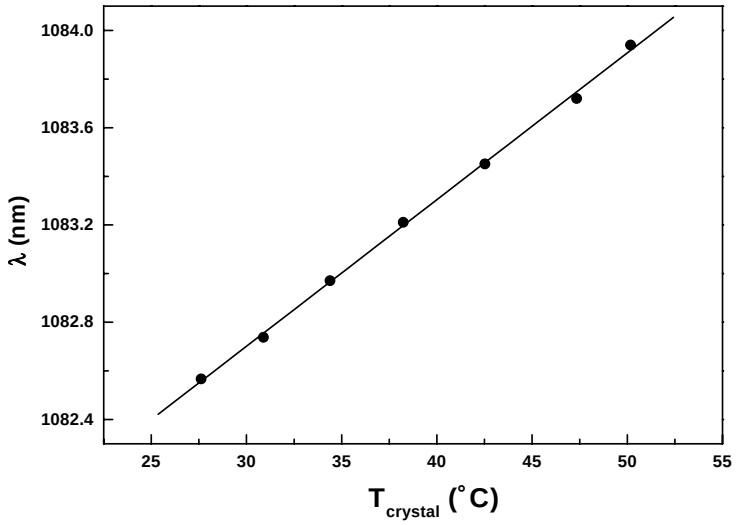

Fig. 5. The plot of wavelength vs. temperature in the QPM conditions for the $\Lambda = 9.50\,\mu m$ domain. The experimental points are fitted with a function $\lambda = [(1080.1 \pm 0.1) + (0.060 \pm 0.001)T]\,nm$ with the temperature in °C.

was found between our results and the Δn calculated from the reported values of $n(T, \lambda)$ for the KTP. This confirms the validity of the wavelength and temperature analysis based on the efficiency curves for a parametric non-linear process as alternative method to measure n variations around the pump or the generated wavelengths. In addition, this analysis demonstrates to be a sensitive and precise way to measure the beam waist of the focused Gaussian beams inside the crystal.

Acknowledgements

We thank M. Inguscio for useful suggestions. A. Arie acknowledges financial support from the European Union under Contract No. ERB FMGECT950017 and Contract No. HPRICT1999-00111. This work was partially supported by Istituto Nazionale di Geofisica e Vulcanologia and Gruppo Nazionale di Vulcanologia, Italy.

References

[1] Fejer MM, Magel GA, Jundt DH, Byer RL. Quasi-phase-matched second harmonic generation: tuning and tolerances. IEEE J Quantum Electron 1992;28:2631–54.
[2] Karlsson H, Laurell F. Electric field poling of flux grown $KTiOPO_4$. Appl Phys Lett 1997;71:3474–6.
[3] Arie A, Rosenman G, Korenfeld A, Skliar A, Oron M, Katz M, Eger D. Efficient resonant frequency doubling of a CW Nd:Yag laser in a bulk periodically poled KTP. Opt Lett 1998;23:28–30.

[4] Arie A, Rosenman G, Mahal V, Skliar A, Oron M, Katz M, Eger D. Green and ultraviolet quasi-phase-matched second harmonic generation in bulk periodically poled $KTiOPO_4$. Opt Commun 1997;142:265–8.
[5] Juwiler I, Arie A, Skliar A, Rosenman G. Efficient quasi-phase-matched frequency doubling with phase compensation by a wedged crystal in a standing-wave external cavity. Opt Lett 1999;24:1236–8.
[6] Wang S, Pasiskevicius V, Laurell F, Karlsson H. Ultraviolet generation by first-order frequency doubling in periodically poled $KTiOPO_4$. Opt Lett 1998;23:1883–5.
[7] Cancio P, Zeppini P, Arie A, De Natale P, Giusfredi G, Rosenman G, Inguscio M. SubDoppler spectroscopy of molecular iodine around 541 nm with a novel solid state laser source. Opt Commun 2000;176:453–8.
[8] Prevedelli M, Cancio P, Giusfredi G, Pavone F, Inguscio M. Frequency control of DBR diode lasers at 1.08 μm and precision spectroscopy of helium. Opt Commun 1996;125:231–6.
[9] Cancio P, Zeppini P, De Natale P, Taccheo S, Laporta P. Noise characteristics of a high-power ytterbium-doped fibre amplifier at 1083 nm. Appl Phys B 2000;70:763–8.
[10] Rosenman G, Skliar A, Eger D, Oron M, Katz M. Low temperature periodic electrical poling of flux-grown $KTiOPO_4$ and isomorphic crystals. Appl Phys Lett 1998;73:3650–2.
[11] Boyd GD, Kleinman DA. Parametric interaction of focused Gaussian light beams. J Appl Phys 1968;39:3597–639.
[12] Kato K. Parametric oscillation at 3.2 μm in KTP pumped at 1.064 μm. IEEE J Quantum Electron. 1991;27:1137–40.
[13] Kato K. Temperature insensitive SHG at 0.5321 μm in KTP. IEEE J Quantum Electron 1992;28:1974–6.
[14] Fradkin K, Arie A, Skliar A, Rosenman G. Tunable midinfrared source by difference frequency generation in bulk periodically poled $KTiOPO_4$. Appl Phys Lett 1999;74:914–6.
[15] Wiechmann W, Kubota S, Fukui T, Masuda H. Refractive-index temperature derivatives of potassium titanyl phosphate. Opt Lett 1993;18:1208–10.
[16] Boulanger B, Fève J, Guillien Y. Thermo-optical effect and saturation of nonlinear absorption induced by gray tracking in a 532-nm-pumped KTP optical parametric oscillator. Opt Lett 2000;25:484–6.